

Nanofluidic control of coupled photonic crystal resonators

Silvia Vignolini,^{1,a)} Francesco Riboli,² Diederik Sybolt Wiersma,¹ Laurent Balet,³ Lianhe H. Li,³ Marco Francardi,⁴ Annamaria Gerardino,⁴ Andrea Fiore,⁵ Massimo Gurioli,² and Francesca Intonti²

¹European Laboratory for Non-linear Spectroscopy, CNR-INO, Via Nello Carrara 1, 50019 Sesto Fiorentino, Italy

²CNISM, Unità di Ricerca di Firenze, Via Sansone 1, 50019 Sesto Fiorentino, Italy and Department of Physics, European Laboratory for Non-linear Spectroscopy, University of Florence, Via Nello Carrara 1, 50019 Sesto Fiorentino, Italy

³Ecole Polytechnique Fédérale de Lausanne, Institute of Photonics and Quantum Electronics, Station 3, CH-1015 Lausanne, Switzerland

⁴Institute of Photonics and Nanotechnology, CNR, via del Cineto Romano 42, 00156 Roma, Italy

⁵COBRA Research Institute, Eindhoven University of Technology, 5600 MB Eindhoven, The Netherlands

(Received 22 December 2009; accepted 11 March 2010; published online 9 April 2010)

A fine control of a photonic molecule is obtained by nanofluidic techniques. The coupling condition between the modes of two photonic crystal nanocavities is modified by spectrally tuning each single resonator. Clear mode anticrossing and transition from localized to delocalized states are observed. The detuning induced by disorder, always present in real device, is experimentally compensated by locally modifying the photonic environment of the cavity. © 2010 American Institute of Physics. [doi:10.1063/1.3378690]

The interaction of two or more coupled resonators is at the basis of many promising issues in the field of photonics¹⁻³ from quantum electrodynamics effects⁴ to slow light engineering.⁵ A class of quantum photonic devices⁶ can be engineered in systems of coupled optical cavities in strong coupling regime with quantum emitters.^{7,8} Within a different scenario, the ability of stopping and storing optical signals has profound implications for optical communications⁹ and for light-matter interaction enhancement.¹⁰ A convenient approach to the experimental realizations of coupled optical resonators relies on two dimensional photonic crystals on membrane.¹¹⁻¹⁶ In such devices, one can exploit microfluidic techniques¹⁷⁻²⁰ to create, control, and tune the properties of photonic crystal based devices and to eventually correct for the presence of fabrication induced disorder.^{21,22}

Here we demonstrate how it is possible, by using different tuning techniques such as local infiltration of water, microevaporation and micro-oxidation, to continuously drive into and out of the coupling condition the modes of two photonic crystals nanocavities by spectrally tuning each single resonator.²³⁻²⁵ Clear mode anticrossing and transition from localized to delocalized states are observed.

The studied structure consists of a two-dimensional triangular lattice of air holes with filling fraction $f=35\%$ and a lattice constant of 320 nm. We chose a defect formed by a hole of 550 nm which replaces a central hole and its six nearest neighbors. The coupling between the two cavities (photonic molecule as defined in Ref. 3) has been studied by using finite-difference time domain (FDTD) code, without including the effects of fabrication-induced disorder.

In Fig. 1(a) we report the two dimensional FDTD calculation of the spectral position of the photonic molecule peaks for two nominally identical cavities at different spatial separations from seven hole (complete uncoupled system) to three hole barriers. In the case of three hole barrier, the split-

ting is large enough to be observed and small enough to be tuned via optofluidic techniques; we thus choose this configuration for our experiment. The sample consists of a GaAs based heterostructure: Three layers of high-density InAs quantum dots emitting at 1300 nm are grown at the center of a 320-nm-thick GaAs membrane.²⁶ A plane-view scanning electron microscope (SEM) image and the calculated three dimensional (3D) FDTD distribution of the electric field intensity associated to the main modes of the photonic molecule are reported in Figs. 1(b) and 1(c), respectively.

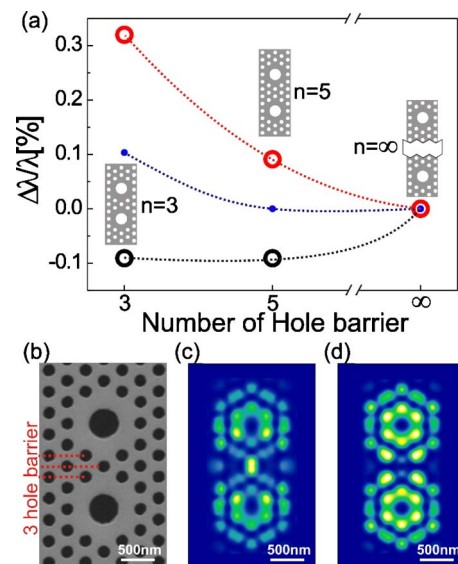


FIG. 1. (Color online) (a) Spectral shift of the photonic molecule peaks as a function of the number of hole planes between the two cavities, calculated by a two-dimensional FDTD model. The black-gray (red) circles represent the symmetric-antisymmetric modes. The small dots are the averaged spectral shifts of the mode of the 550 nm cavity when coupled with either 500 or 600 nm cavities, and they represent the nonresonant mode shift. (b) SEM image of the studied sample, with three hole barrier separation. [(c) and (d)] Spatial distribution of the electric field intensity associated to the symmetric and antisymmetric mode, respectively, as calculated by 3D FDTD model.

^{a)}Electronic mail: vignolini@lens.unifi.it.

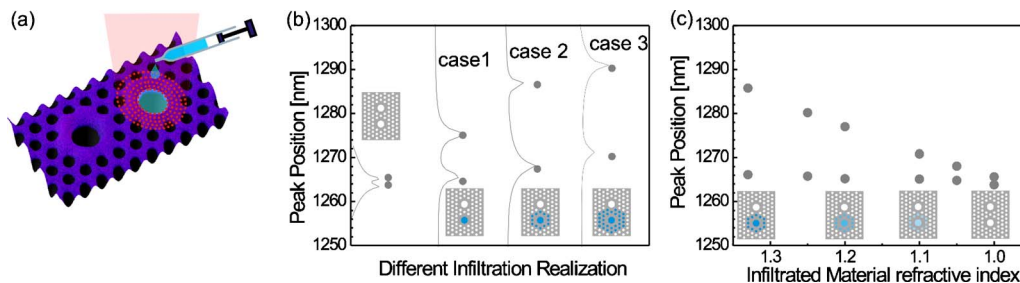


FIG. 2. (Color online) (a) Schematic description of the tuning method. (b) FDTD calculations for different infiltration configurations. (c) FDTD calculations for different fine tuning configurations. The evaporation is simulated by reducing the refractive index of the infiltrated material. The value of the refractive index is decreased from $n=1.33$ (filled cavity) to $n=1$ (empty cavity).

In order to vary the coupling between the main modes of the two interacting cavities we modify one of the two resonators by locally infiltrating its central hole with water. A description of the method is sketched in Fig. 2(a). At room temperature the infiltrated water remains in the pores, but as the sample is heated via laser excitation, the water evaporation could be induced and a control of the evaporation rate could be exploited to fine tune the cavity resonances.²⁵ The results of a 3D FDTD calculations of the photonic molecule modes are shown in Fig. 2(b), for different selective infiltrations (case 1, 2, and 3). The spectrum of the not-infiltrated system shows two coupled modes separated by 2 nm. The infiltration with water destroys the coupling due to the large detuning of the infiltrated cavity mode. Case 1 refers to the infiltration of only the central 550 nm hole, case 2 refers to the additional infiltration of the first ring of 12 pores surrounding the cavity, and case 3 refers to the further infiltration of the second ring of 16 pores. Due to the lack of knowledge on the details of the water configuration after partial evaporation, we simulated the partial filling of the holes via a reduction in the effective refractive index of the infiltrated liquid. The results of the 3D FDTD calculations are reported in Fig. 2(c) for a specific infiltration condition, that is by filling the 550 nm hole and the first ring of hole surrounding it [case 2 of Fig. 2(b), which likely corresponds to the experimental realization discussed below].

Photoluminescence (PL) spectra and two dimensional PL maps of the samples are obtained with a confocal microscope with a spatial resolution of 1 μm . The sample is excited with light from a diode laser ($\lambda=780$ nm, excitation

density of 0.25 MW/cm^2) and the emitted PL signal is coupled to a single-mode optical fiber, acting as a confocal pinhole, connected to a spectrometer. The PL signal, dispersed by the spectrometer, is finally collected by a liquid nitrogen cooled InGaAs array (spectral resolution of 1 nm). Before the infiltration we measured a mode splitting of (3.90 ± 0.05) nm, which is larger than the 3D FDTD theoretical splitting of 2 nm, likely denoting the presence of photonic disorder.

A local infiltration apparatus permits to perform a controlled liquid deposition inside the central hole of one of the two cavities that form the photonic molecule. The heating of the sample is provided by the same PL setup at high excitation density.²⁵ Our spatial resolution of 1 and the 1.3 μm separation between the two cavities, allows us to perform a local heating of the infiltrated region. In addition, we focused the laser 500 nm off from the center of the infiltrated cavity, along the coupling axis and far from the not-infiltrated cavity. The laser excitation causes an increase in the temperature that in turn raises the value of the dielectric constant. This gives a red shift of the PL peaks under high excitation and we use it to control the sample temperature during the heating.²⁵

After the heating treatment we kept the sample in the dark for several minutes to cool it down, then PL spectra at low excitation are collected in order to monitor the stages of the cavity detuning. Typical data are reported in Fig. 3, where the top panels show the maps of the short (S) and long (L) wavelength mode and the low panels show the PL spec-

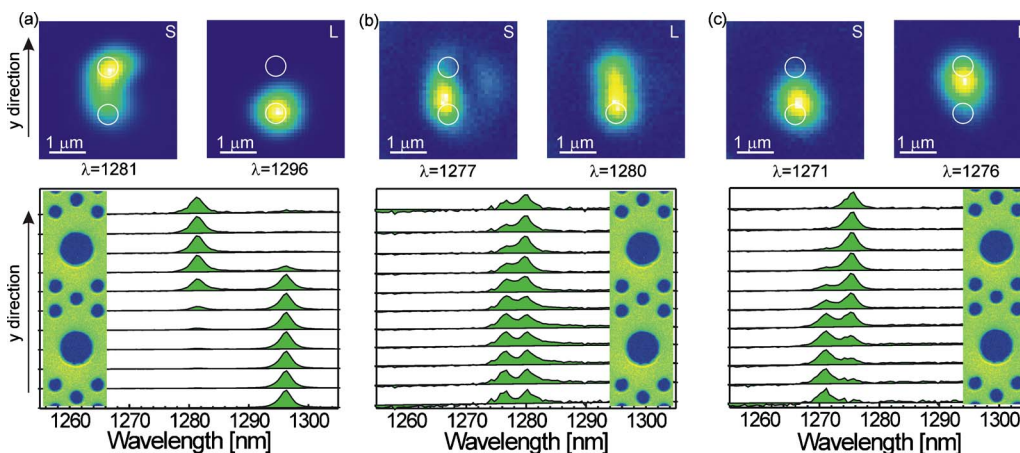


FIG. 3. (Color online) The two top panels show the photoluminescence map for the two modes of the system at short (S) and long (L) wavelengths. In the low panel the spectra for different positions (step of 200 nm) along the vertical direction of the photonic molecule are reported. The SEM images reported in the low panels are scaled in order to give the spatial position of each spectrum. (a) Data after the infiltration process. (b) Data at zero detuning. (c) Data with negative detuning.

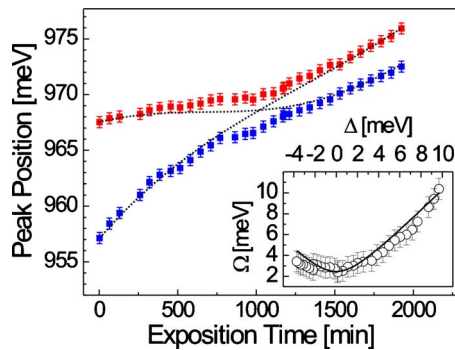


FIG. 4. (Color online) Peaks position behavior during the detuning variation via local heating. Dotted lines are fits of the mode energies far from the coupling region. Inset: mode splitting as a function of Δ , as estimated from the fits.

tra collected in different positions along the vertical axis of the photonic molecule (y-direction). Figure 3(a) reports the PL map and the PL spectra of the molecule modes just after the infiltration process. In this case the two modes are separated by 18 nm and each of them is clearly localized on a well defined cavity; therefore, the induced shift is so large to completely destroy the coupling in the photonic molecule. By comparing the experimental PL spectra before and after the infiltration process with the prediction of the FDTD calculation, we conclude that we infiltrated the bottom defect and the first ring of holes surrounding it. By increasing the excitation density to 1.3 MW/cm² we are able to force the water to evaporate at a very slow rate. Even if our excitation power is quite low with respect to the one used in Ref. 27 to induce the GaAs oxidation, we found that the exposition time is long enough to produce a non-negligible oxidation of the slab. This process contributes with an additional PL blue shift of the modes and the two effects of microevaporation and micro-oxidation cannot be easily separated. Measurements in a single cavity without infiltrated water, however show that the PL blueshift due to the oxidation is not the major effect.

Finally we reach the condition where the splitting between the two PL peaks is minimum (3.15 ± 0.05 nm) and the corresponding maps of the peaks and the spectra are reported in Fig. 3(b). This value is larger than the one predicted by FDTD calculation for the empty cavities, but the discrepancy cannot be associated to a residual detuning as shown by the clear anticrossing of the data and the spatial maps of the modes. We believe that the likely explanation of the experimental splitting is due to the presence of water in the holes between the cavities, that increases the coupling energy. By continuing the local heating, we were able to invert the sign of the detuning; such inversion cannot be achieved with the microevaporation method and it is a clear signature of the micro-oxidation process. As shown in Fig. 3(c), by changing the sign of the detuning we exchange the spatial localization of the modes of the photonic molecule, as expected.

In Fig. 4, where the spectral positions of the PL peaks are reported as a function of the exposition time of the laser heating, a clear anticrossing behavior is observed. The experimental value of the minimum splitting, 2.4 ± 0.1 meV, is in agreement with the results of the FDTD calculations, if the presence of a partially infiltrated pore in between the two cavities is considered. At room temperature, each defined

configuration of detuning is stable in time. The difference between the experimental PL peak energies of the two modes Ω is reported in the inset of Fig. 4 as a function of the detuning Δ . By using the standard formula for two coupled modes $\Omega = \sqrt{\Delta^2 + 4g^2}$, where g is the coupling energy of the modes, we fitted the experimental data obtaining $g = 1.2 \pm 0.2$ meV.

We acknowledge financial support from the FAR under Project No. 851 and Ente Cassa di Risparmio di Firenze.

- ¹M. T. Hill, H. J. S. Dorren, T. de Vries, X. J. M. Leijtens, J. H. den Besten, B. Smalbrugge, Y. S. Oei, H. Binsma, G.-D. Khoe, and M. K. Smit, *Nature (London)* **432**, 206 (2004).
- ²T. Mukaiyama, K. Takeda, H. Miyazaki, Y. Jimba, and M.-K. Gonokami, *Phys. Rev. Lett.* **82**, 4623 (1999).
- ³M. Bayer, T. Gutbrod, J. P. Reithmaier, A. Forchel, T. L. Reinecke, P. A. Knipp, A. A. Dremin, and V. D. Kulakovskii, *Phys. Rev. Lett.* **81**, 2582 (1998).
- ⁴A. D. Greentree, C. Tahan, J. H. Cole, and L. C. L. Hollenberg, *Nat. Phys.* **2**, 856 (2006).
- ⁵T. Baba, *Nat. Photonics* **2**, 465 (2008).
- ⁶D. Gerace, H. E. Tureci, A. Imamoglu, V. Giovannetti, and R. Fazio, *Nat. Phys.* **5**, 281 (2009).
- ⁷T. Yoshie, A. Scherer, J. Hendrickson, G. Khitrova, H. M. Gibbs, G. Rupper, C. Ell, O. B. Shchekin, and D. G. Deppe, *Nature (London)* **432**, 200 (2004).
- ⁸K. Hennessy, A. Badolato, M. Winger, D. Gerace, M. Atature, S. Gulde, S. Falt, E. L. Hu, and A. Imamoglu, *Nature (London)* **445**, 896 (2007).
- ⁹D. Englund, A. Faraon, B. Zhang, Y. Yamamoto, and J. Vučković, *Opt. Express* **15**, 5550 (2007).
- ¹⁰B. Corcoran, C. Monat, C. Grillet, D. J. Moss, B. J. Eggleton, T. P. White, L. O'Faolain, and T. F. Krauss, *Nat. Photonics* **3**, 206 (2009).
- ¹¹H. Altug, D. Englund, and J. Vuckovic, *Nat. Phys.* **2**, 484 (2006).
- ¹²D. O'Brien, M. D. Settle, T. Karle, A. Michaeli, M. Salib, and T. F. Krauss, *Opt. Express* **15**, 1228 (2007).
- ¹³S. Vignolini, F. Intonti, M. Zani, F. Riboli, D. S. Wiersma, L. H. Li, L. Balet, M. Francardi, A. Gerardino, A. Fiore, and M. Gurioli, *Appl. Phys. Lett.* **94**, 151103 (2009).
- ¹⁴K. A. Atlasov, K. F. Karlsson, A. Rudra, B. Dwir, and E. Kapon, *Opt. Express* **16**, 16255 (2008).
- ¹⁵S. V. Zhukovsky, D. N. Chigrin, A. V. Lavrinenko, and J. Kroha, *Phys. Rev. Lett.* **99**, 073902 (2007).
- ¹⁶D. P. Fussell and M. M. Dignam, *Appl. Phys. Lett.* **90**, 183121 (2007).
- ¹⁷D. Erickson, T. Rockwood, T. Emery, A. Scherer, and D. Psaltis, *Opt. Lett.* **31**, 59 (2006).
- ¹⁸M. Lončar, A. Scherer, and Y. Qiu, *Appl. Phys. Lett.* **82**, 4648 (2003).
- ¹⁹C. L. C. Smith, D. K. C. Wu, M. W. Lee, C. Monat, S. Tomljenovic-Hanic, C. Grillet, B. J. Eggleton, D. Freeman, Y. Ruan, S. Madden, B. Luther-Davies, H. Giessen, and Y.-H. Lee, *Appl. Phys. Lett.* **91**, 121103 (2007).
- ²⁰C. Monat, P. Domachuk, and B. J. Eggleton, *Nat. Photonics* **1**, 106 (2007).
- ²¹B. M. Möller, U. Woggon, and M. V. Artemyev, *Phys. Rev. B* **75**, 245327 (2007).
- ²²M. Benyoucef, S. Kiravittaya, Y. F. Mei, A. Rastelli, and O. G. Schmidt, *Phys. Rev. B* **77**, 035108 (2008).
- ²³F. Intonti, S. Vignolini, V. Turck, M. Colocci, P. Bettotti, L. Pavesi, S. L. Schweizer, R. Wehrspohn, and D. S. Wiersma, *Appl. Phys. Lett.* **89**, 211117 (2006); D. S. Wiersma, S. Vignolini, V. Tuerk, and F. Intonti, Patent No. WO2007/107959 A1 (2007).
- ²⁴S. Vignolini, F. Riboli, F. Intonti, M. Belotti, M. Gurioli, Y. Chen, M. Colocci, L. C. Andreani, and D. S. Wiersma, *Phys. Rev. E* **78**, 045603 (2008).
- ²⁵F. Intonti, S. Vignolini, F. Riboli, M. Zani, D. S. Wiersma, L. Balet, L. H. Li, M. Francardi, A. Gerardino, A. Fiore, and M. Gurioli, *Appl. Phys. Lett.* **95**, 173112 (2009).
- ²⁶M. Francardi, L. Balet, A. Gerardino, C. Monat, C. Zinoni, L. H. Li, B. Alloing, N. Le Thomas, R. Houdré, and A. Fiore, *Phys. Status Solidi C* **3**, 3693 (2006).
- ²⁷H. S. Lee, S. Kiravittaya, S. Kuma, J. D. Plumhof, L. Balet, L. H. Li, M. Francardi, A. Gerardino, A. Fiore, A. Rastelli, and O. G. Schmidt, *Appl. Phys. Lett.* **95**, 191109 (2009).